Saudi Pharmaceutical Journal 28 (2020) 172–186

Contents lists available at ScienceDirect

Saudi Pharmaceutical Journal

journal homepage: www.sciencedirect.com

Original article

Cell proliferation activity delineated by molecular docking of four new compounds isolated from the aerial parts of *Suaeda monoica* Forssk. ex. J. F. Gmel

Nasir A. Siddiqui [a], Ramzi A. Mothana [a,*], Mansour S. Al-Said [a], Mohammad K. Parvez [a], Perwez Alam [a], M. Tabish Rehman [a], Mohd. Ali [b], Mohamed F. Alajmi [a], Mohammed S. Al-Dosari [a], Adnan J. Al-Rehaily [a], Fahd A. Nasr [c], Jamal M. Khalid [d]

[a] Department of Pharmacognosy, College of Pharmacy, King Saud University, Riyadh, Saudi Arabia
[b] Department of Pharmacognosy & Phytochemistry, Faculty of Pharmacy, Jamia Hamdard, New Delhi, India
[c] Medicinal Aromatic, and Poisonous Plants Research Center, Department of Pharmacognosy, College of Pharmacy, King Saud University, Riyadh, Saudi Arabia
[d] Department of Botany and Microbiology, College of Science, King Saud University, Riyadh, Saudi Arabia

ARTICLE INFO

Article history:
Received 6 August 2019
Accepted 29 November 2019
Available online 7 December 2019

Keywords:
Suaeda monoica
Cell-proliferation
Molecular docking
β-Naphthol
Caproic acid
Chenopodiaceae
HepG2 cells

ABSTRACT

Using different chromatographic methods, four new compounds were isolated from the aerial parts of *Suaeda monoica* (Chenopodiaceae) along with 2-hydroxy-1-naphthoic acid (SCM-3). The structures of the new compounds were established as 6′-hydroxy-10′-geranilanyl naphtha-1-oate (SMC-1), 4,4,8β,10β-Tetramethyl-9β-isobutanyl decalin-13-ol-13-O-β-D-xylopyranoside (SCM-2), 6′-(2-hydroxy naphthalen-3-yl) hexanoic acid (SCM-4) and 1′-(2-Methoxy-3-naphthyl)-4′-(2′′-methylbenzoyl)-*n*-butane (SMC-5) by IR, EIMS and NMR (1 & 2D) analyses. All compounds (50 μg/mL) were tested for cell proliferative potential on cultured human liver cell HepG2 cells by MTT assay. The results revealed a marked cell proliferative potential of all compounds (1.42–1.48 fold) as compared to untreated control. The results of molecular docking and binding with specific proteins such as PTEN (Phosphatase and Tensin homolog) and p53 also justify the cell proliferative potential of the isolated compounds. Glide program with Schrodinger suit 2018 was used to evaluate the binding between SMC compounds and proteins (PTEN and p53). The binding affinity of all compounds was in order of 10^4–10^5 M^{-1} towards both PTEN and p53. All the SMC compounds have been found to bind at the active site of PTEN, thereby may prevent the binding of phosphatidylinositiol 3,4,5-triphosphate (PI3P). In the locked position, PTEN would not be able to hydrolyze PI3P and hence the PI3P regulated signaling pathway remains active. Similarly, SMC molecules were found to interact with the amino acid residues (Ser99, Thr170, Gly199, and Asp224) which are critically involved in the formation of tetrameric p53. The blockage of p53 to attain its active conformation thus may prevent the recruitment of p53 on DNA and hence may promote cell proliferation.

1. Introduction

Genus *Suaeda* belongs to halophytes category from the family Chenopodiaceae, consisting of around 75 species widely distributed around seacoasts, salty marshes and deserts (Boulos, 1991). *Suaeda monoica* Forssk. ex. J.F. Gmel (SMC) is a bushy dark green succulent leaved shrub with pale green flowers. In Saudi Arabia genus *Suaeda* is represented by nine species (Boulos, 1999) out of which five are found in Al Jouf area (*S. aegyptica*, *S. vera*, *S. vermiculata*, *S. fruticosa* and *S. mollis* (Al-Hassan, 2006) while *S.*

* Corresponding author at: Department of Pharmacognosy, College of Pharmacy, King Saud University, P.O. BOX 2457, Riyadh 11451, Saudi Arabia.
E-mail address: rmothana@ksu.edu.sa (R.A. Mothana).

Peer review under responsibility of King Saud University.

Production and hosting by Elsevier

https://doi.org/10.1016/j.jsps.2019.11.019
1319-0164/

monoica distributed in the southern lowlands and sometimes forming a tree of approx. 3 m height (Collenette, 1999).

Mangrove plants have already established their identity as one of the useful category of medicinal plants in traditional system of medicine (Premnathan et al., 1992; Premnathan et al., 1996). Antiviral, wound healing and hepatoprotective potential of *S. monoica* leaves have also been reported (Ravikumar et al., 2010; Ravikumar et al., 2011a). Earlier reports proved the medicinal potential of *S. monoica* against *Plasmodium falciparum*, insects and microbes (Chandrasekaran et al., 2008; Kassem et al. 2003; Ravikumar et al., 2011b). The existing literature reports the presence of a broad range of chemical constituents in *S. monoica* such as proteins, tannins, resins, terpenoids, glycosides and flavonoids (Lakshmanan et al., 2013). From the phytochemical point of view, the major classes of compounds reported in *S. monoica* are different fatty acids, triterpenoids and sterols (Chandrasekaran et al., 2008; Bandaranayake 1998; Yezhelyev et al., 2006). A polysaccharide which is active against human immune deficiency virus also reported from *S. monoica* (Premnathan et al., 1992; Padmakumar et al., 1997). The recent phytochemical findings suggest the presence of gallic acid, catechin, caffeic acid, syringic acid, rutin, coumaric acid, vanillin and quercetin in methanolic extract of aerial parts of *S. monoica and S. pruinosa* (Elsharabasy et al., 2019). Elsharabasy et al also reported the presence of several amino acids in both the species. These amino acids include histidine, arginine, threonine, alanine, proline, tyrosine, methionine, cysteine, isoleucine, leucine, lysine, aspartic acid, glutamic acid and glycine in *S. monoica and S. pruinosa*. Several fatty acids such as lauric acid, myristoleic acid, palmitic acid, palmitoleic acid, stearic acid, oleic acid, linoleic acid and linolenic acid were also identified in *S. monoica and S. pruinosa* by Elsharabasy et al., 2019. A norsesquaterpenol named as 13,17-octahydropentalene-4,4,10,23-tetramethyl-17,21-diisopropyltetradecahydrocyclo-[a]-phenanthrene-(14), 20(23), 21(30)-trien-5a-ol and a monocyclic triterpenoid named as [1,4,4-trimethylcyclopent- 1(5)-enyl]-9,10,17,21-tetramethyl-9a-ol-16a (17a)-epoxy heptadecan-6,10-dione along with 3-epi-lupeol and 4-cyclopentylpyrocatechol were reported by Al-Said et al., 2017 in ethanolic extract of aerial parts of *S. monoica*.

Natural products play a vital role in healing, protection and rejuvenation of the tissues probably by enhancing the cell division and ultimately leading to cell proliferation. Natural products have well established history of healing and regenerative potential for various tissues in human body (Hasan and Al Sorkhy, 2014). Several herbal drugs have been utilized in the treatment of disease arise due to decline of stem cell proliferation and utilized for regeneration and rehabilitation of tissues by promoting cell proliferation. The essential obligation of cell proliferation is in tissue regeneration, repair and aging (Al-Said et al., 2017). Herbal extracts also stimulated skin cells growth like hyperforin from *Hypericum perforatum* stimulated keratinocyte differentiation, polysaccharides in *Actinidia chinensis* stimulated human keratinocytes and other herbal extracts induce dermal papilla cells proliferation (Ashtiani et al., 2012). Taking into consideration the demand of cell proliferative agents, this study was planned to explore cell proliferative effect of various phytoconstituents isolated from *S. monoica* because till now *S. monoica* phytoconstituents have not been extensively explored.

The cell proliferative potential of *S. monoica* was investigated against HepG2 cells by MTT assay. Furthermore, a bioassay guided fractionation and isolation was carried out to isolate four new compounds (SMC-1, -2, -4, -5) along with a known compound (SMC-3). In addition, molecular docking studies by binding them to PTEN and p53 proteins using AutoDock 4.2 were performed to assure the cell proliferation effect (AlAjmi et al., 2018).

2. Materials and methods

2.1. Instruments

Infrared spectra were recorded from ATI Mattson genesis series Fourier transform (FT-IR) infrared spectrophotometer. Bruker Avance DRX 500 MHz spectrometer (Massachusetts, United States) was used to obtain 1D and 2D NMR spectra at 500 and 125 MHz for ^{1}H and ^{13}C, respectively. Bruker Bioapex FT–MS (Massachusetts, United States) was used to obtain the EI mass spectra.

2.2. Plant material

The collection of *S. monoica* (aerial parts) was done in March 2017 from Aqabaat Al-Makhwah, after tunnel # 13, Saudi Arabia. The Identification of the plant was done by Field Taxonomist, Pharmacognosy Department, College of Pharmacy, KSU, Riyadh. Voucher Specimen (Voucher # 15235) was deposited in herbarium of Pharmacognosy Department.

2.3. Extraction and isolation of phytoconstituents

The aerial parts of *S. monoica* were dried in air and ground to coarse powder (1150 g) and, then extracted by percolation using ethanol (95%) as extractive solvent. Extraction was repeated for three times (3 × 2 L) to complete exhaustion of the plant material, then all cuts were combined and concentrated in rotary vacuum evaporator to get 60 g of a dried semi solid extract. The total amount of the extract was dissolved in hot MeOH and left for overnight, then filtered off to afford a dry soluble portion of 40 g and a fatty-nature solid. This 40 g of the extract was processed as mentioned in the scheme of isolation. After multiple and stepwise partitioning of the total amount of the extract, fractions **A** (*n*-hexane), **B** (dichloromethane), **C** (ethyl acetate) and **D** (*n*-butanol) were produced (Scheme 1). The ethyl acetate-fraction (fraction **C**, 1.2 g) was separated utilizing column chromatography on sephadex LH-20 column (20 mm i.d. × 400 mm) to give 5 fractions (**C1-C5**). The elution was performed with methanol: water (9:1). Fraction **C4** showed a major compound, which was purified on a sephadex LH-20 column) (15 mm i.d. × 600 mm) with methanol: water (9:1) to afford **SMC-1** (25 mg). The dichloromethane-fraction (fraction **B**, 1.8 g) was subjected to a pre-packed silica gel column (35 mm i.d. × 400 mm) using a gradient of dichloromethane: methanol (100:1) to pure methanol as a mobile phase to afford 10 fractions (**B1-B10**). Fraction **B3** was eluted with dichloromethane and methanol (19:1) using sephadex LH-20 column (10 mm i.d. × 600 mm) to afford **SMC-2** (14 mg). The purification of the major compound in fraction **B6** utilizing sephadex LH-20 column (10 mm i.d. × 600 mm) with dichloromethane and methanol (9:1) as an eluent, gave **SMC-3** (11 mg). The isolation of **SMC-4** (6 mg) was achieved from fraction **B7** utilizing sephadex LH-20 column (10 mm i.d. × 600 mm) with dichloromethane and methanol (9:1) as a solvent. **SMC-5** (8 mg) was isolated from fraction **B8** by eluting with dichloromethane and methanol (5:1) using sephadex LH-20 column (10 mm i.d. × 600 mm).

2.3.1. 6′-hydroxy-10′-geranilanyl naphtha-1-oate (SMC-1)

It was a yellow semisolid compound isolated from the ethyl acetate fraction. IR υ^{max} (KBr): 3360, 2964, 1737, 1614, 1519, 1434, 1361, 1197, 1064, 979, 783, 745 cm^{-1}; ^{1}H NMR (CD_3OD): δ 6.62 (1H, m, H-2), 6.60 (2H, m, H-6, H-9), 6.58 (1H, m, H-4), 6.45 (1H, m, H-3), 6.41 (1H, m, H-7), 6.38 (1H, m, H-8), 4.01 (1H, d, J = 7.5 Hz, H_2-10′a), 3.95 (1H, d, J = 7.0 Hz, H_2-10′b), 3.52 (1H, m, $w_{1/2}$ = 7.5 Hz, H-6′β), 2.63 (2H, m, H_2-5′), 2.54 (1H, m, H-3′), 2.50

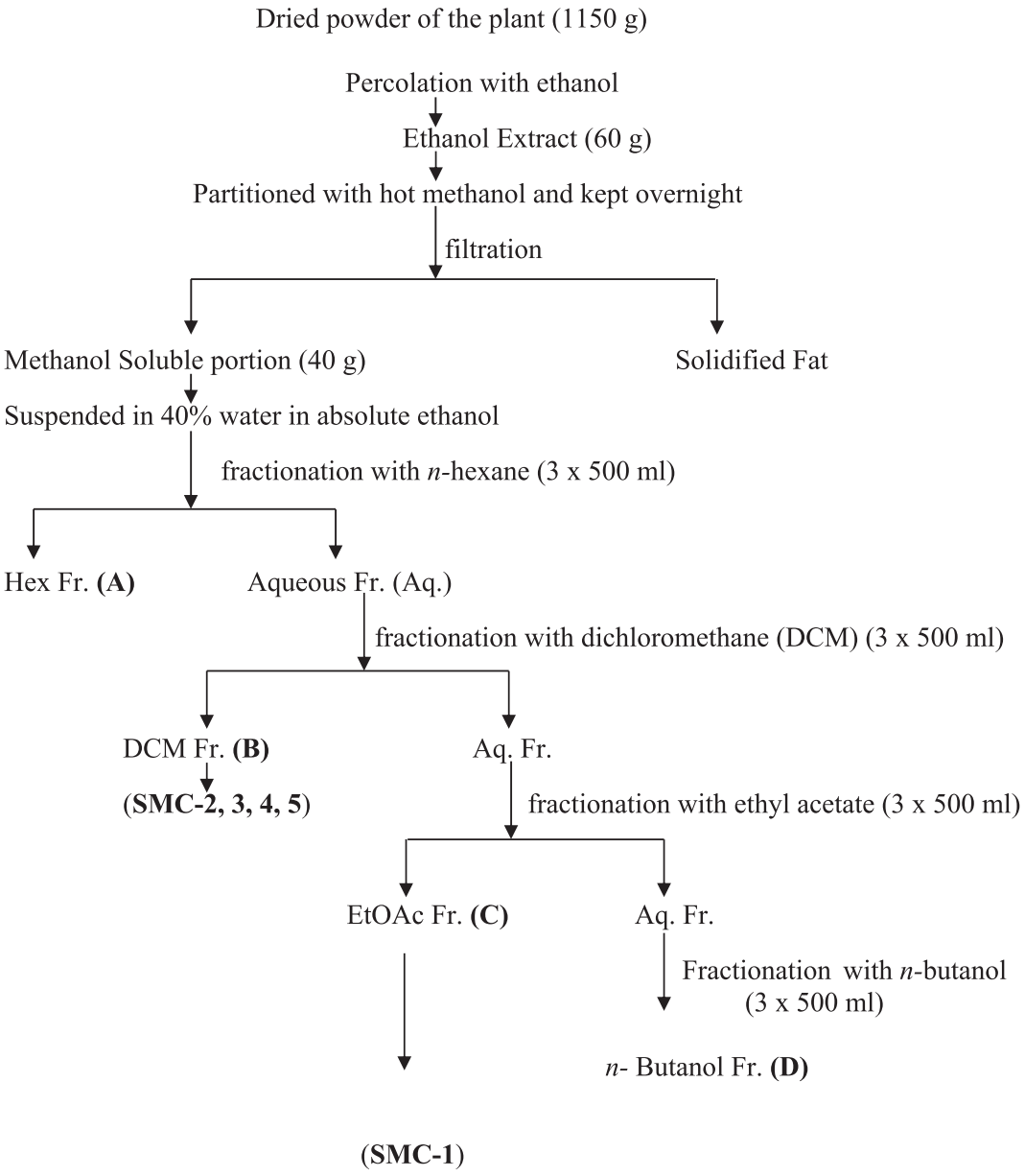

Scheme 1. Isolation scheme of SMC compounds.

(1H, m, H-7′), 1.88 (2H, m, H_2-4′), 1.38 (2H, m, H-6, H_2-2′), 1.25 (3H, d, *J* = 6.5 Hz, Me-8′), 1.23 (3H, d, *J* = 6.3 Hz, Me-9′), 0.84 (3H, t, *J* = 6.5 Hz, Me-1′); ^{13}C NMR (CD_3OD): δ 130.40 (C-1), 121.25 (C-2), 121.32 (C-3), 131.80 (C-4), 132.63 (C-5), 126.52 (C-6), 117.01 (C-7), 116.32 (C-8), 130.82 (C-9), 131.16 (C-10), 169.13 (C-11), 9.65 (C-1′), 22.42 (C-2′), 49.21 (C-3′), 30.26 (C-4′),36.21 (C-5′), 70.10 (C-6′), 39.66 (C-7′), 20.85 (C-8′), 21.13 (C-9′), 64.62 (C-10′); EIMS *m*/*z* (rel. int.): 328 [M]+ ($C_{21}H_{28}O_3$) (1.1), 285 (2.5), 173 (4.2), 157 (9.2), 155 (44.8), 141 (1.2), 123 (100).

2.3.2. 4,4,8β,10β-Tetramethyl-9β-isobutanyl-13-ol-13-β-D-xylopyranoside (SMC-2)

It was a colorless solid compound isolated from dichloromethane fraction. IR υ^{max} (KBr): 3415, 3392, 2958, 2867, 1458, 1367, 1164, 1074, 1024 cm^{-1}; ^{1}H NMR (DMSO d_6): δ 4.23 (1H, d, *J* = 7.5 Hz, H-1′), 3.51 (1H, dd, *J* = 6.2, 1.1 Hz, H_2-13a), 3.42 (1H, dd, *J* = 6.3, 1.1 Hz, H_2-13b), 3.40 (1H, m, H-4′), 3.23 (1H, dd, H-2′), 3.09 (1H dd, J = 7.1, 1.2 H_2-5′a), 3.06 (2H,dd, *J* = 6.9, 1.2 Hz, H_2-5b'), 3.02 (1H, dd, H-3′), 2.89 (1H, m, H-12), 2.21 (1H, m, H-9), 1.89 (2H, m, H_2-1), 1.80 (2H, m, H_2-7), 1.51 (1H, m, H-5), 1.47 (2H, m, H_2-2), 1.20 (2H, m, H_2-3), 1.14 (2H, m, H_2-6), 0.96 (2H, m, H_2-11), 0.90 (3H, s, Me-17), 0.82 (3H, s, Me-15), 0.76 (3H, d, *J* = 6.1 Hz, Me-18), 0.73 (3H, d, *J* = 6.5 Hz, Me-16), 0.65 (3H, s, Me-14); ^{13}C NMR (DMSO d_6): δ 35.91 (C-1), 32.63 (C-2), 30.22 (C-3), 46.22 (C-4), 57.18 (C-5), 29.75 (C-6), 42.35 (C-7), 45.08 (C-8), 56.23 (C-9), 35.18 (C-10), 25.48 (C-11), 49.56 (C-12), 61.04 (C-13), 11.74 (C-14), 18.90 (C-15), 19.06 (C-16), 19.68 (C-17), 18.58 (C-18), 101.25 (C-1′), 73.82 (C-2′), 76.71 (C-3′), 70.04 (C-4′), 66.15 (C-5′); EIMS *m*/*z* (rel. int.): 398 [M]+ ($C_{23}H_{42}O_5$) (100), 383 (22.7), 368 (6.3), 234 (3.2), 205 (8.3), 163 (5.2), 149 (28.5), 133 (30.2).

2.3.3. 6′-(2-hydroxynaphthalen-3-yl)hexanoic acid (SMC-4)

It was a yellow amorphous solid compound isolated from dichloromethane fraction. IR υ^{max} (KBr): 3407, 3209, 2971, 2852, 1677, 1521, 1471, 1355, 1296, 1272, 1228, 1108, 775 cm^{-1}; ^{1}H NMR (CD_3OD): δ 6.95 (1H, dd, *J* = 7.3, 2.0 Hz, H-9), 6.73 (1H, s,

H-1), 6.69 (1H, d, J = 8.0, 1.3 Hz, H-6), 6.60 (1H, s, H-4), 6.45 (1H, m, H-8), 6.02 (1H, m, H-7), 2.86 (2H, t, J = 7.5 Hz, H_2-6′), 2.42 (2H, t, J = 7.5 Hz, H_2-2′), 2.29 (2H, m, H_2-5′), 1.58 (2H, m, H_2-4′), 1.27 (2H, m, H_2-3′); ^{13}C NMR (CD_3OD): δ 124.80 (C-1), 164.56 (C-2), 131.12 (C-3), 127.10 (C-4), 129.10 (C-5), 120.62 (C-6), 117.02 (C-7), 118.14 (C-8), 127.82 (C-9), 131.70 (C-10), 178.37 (C-1′), 38.66 (C-2′), 26.04 (C-3′), 30.02 (C-4′), 35.10 (C-5′), 52.10 (C-6′); EIMS m/z (rel. int.): 258 [M]+ ($C_{16}H_{18}O_3$) (2.3).

2.3.4. 1′-(2-Methoxy-3-naphthyl)-4′-(2′′-methylbenzoyl)-n-butane (SMC-5)

It was a yellow crystalline compound isolated from dichloromethane fraction. IR υ^{max} (KBr): 2927, 2851, 1733, 1637, 1596, 1515, 1269, 1031, 979, 848 cm^{-1}; ^{1}H NMR (CD_3OD): δ 7.46 (1H, dd, J = 10.5, 2.3 Hz, H-6′′), 7.12 (1H, s, H-1), 7.06 (1H, dd, J = 9.0, 1.0 Hz, H-3′′), 7.04 (1H, dd, J = 8.5, 1.0 Hz, H-6), 6.82 (1H, dd, J = 8.1, 1.5 Hz, H-9), 6.75 (2H, m, H-7, H-4′′), 6.45 (2H, m, H-8, H-5′′), 6.41 (1H, s, H-4), 3.85 (3H, s, OCOMe), 3.46 (2H, t, J = 7.5 Hz, H_2-1′), 3.37 (3H, s, OMe), 3.33 (2H, t, J = 7.3 Hz, CH_2-4′), 2.78 (2H, m, H_2-3′), 1.26 (2H, m, H_2-2′); ^{13}C NMR (CD_3OD): δ 123.43 (C-1), 156.61 (C-2), 123.38 (C-3), 128.01 (C-4), 130.32 (C-5), 121.02 (C-6), 116.41 (C-7), 118.81 (C-8), 128.21 (C-9), 130.95 (C-10), 49.67 (C-1′), 35.73 (C-2′), 42.59 (C-3′), 42.71 (C-4′), 132.24 (C-1′′), 130.48 (C-2′′), 128.37 (C-3′′), 118.75 (C-4′′), 118.66 (C-5′′), 132.19 (C-6′′), 169.47 (C-7′′), 56.57 (OCOMe), 50.01 (OMe); EIMS m/z (rel. int.): 348 [M]+ ($C_{23}H_{24}O_3$) (1.1), 333 (11.9), 317 (14.5), 258 (8.3), 191 (100), 177 (72.8), 163 (2.8), 149 (4.6), 135 (7.5), 120 (43.9), 105 (3.7), 77 (13.9).

2.3.5. 2-Hydroxy-1-naphthoic acid (SMC-3)

It was a yellow amorphous solid compound isolated from dichloromethane fraction with m. p. 220–222 °C. IR υ^{max} (KBr): 3377, 3221, 2948, 2851, 1670, 1611, 1512, 1448, 1328, 1313, 1244, 1216, 1172, 977, 833 cm^{-1}; ^{1}H NMR (CD_3OD): δ 7.59 (1H, d, J = 9.7 Hz, H-3), 7.44 (1H, d, J = 9.0 Hz, H-6), 7.42 (1H, d, J = 9.0 Hz, H-9), 6.84 (1H, m, H-7), 6.82 (1H, m, H-8), 6.60 (1H, s, OH), 6.30 (1H, d, J = 9.7 Hz, H-4); ^{13}C NMR (CD_3OD): δ 131.28 (C-1), 160.93 (C-2), 131.85 (C-3), 131.21 (C-4), 131.05 (C-5), 127.33 (C-6), 115.56 (C-7), 116.26 (C-8), 127.53 (C-9), 131.19 (C-10), 171.49 (C-11); EIMS m/z (rel. int.): 188 [M]+ ($C_{11}H_8O_3$) (1.1).

2.4. Cell proliferation assay

Human hepatoblastoma cells, HepG2 were maintained in RPMI-1640 medium (Gibco, USA), supplemented with 10% bovine serum (Gibco, USA) and 1 × penicillin–streptomycin mixture (Invitrogen, USA) and incubated at 37 °C with 5% CO_2 supply in a humid chamber. HepG2 cells (0.5 × 10^5/well) were seeded in a 96-well flat-bottom plate (Becton-Dickinson Labware, USA) and incubated overnight. Stock solutions of compounds (SMC-1, SMC-2, SMC-3, SMC-4 and SMC-5; 1 mg, each) were prepared by first dissolving in 50 µL DMSO and then in RPMI medium (1 mg/mL; DMSO > 0.1%, final), followed by reconstitution of four working concentration (50, 25, 12.5 and 6.25, µg/mL) in the medium. DMSO vehicle or untreated control was also included.

For cell proliferation assay (TACS MTT Cell Proliferation Assay Kit, Tervigen, USA), the cells were treated with the four different doses of SMC-compounds, including control in triplicate. After 48 h of incubation, MTT reagent (10 µL/well) was added to each well and incubated at room-temperature for 4 h in dark. Immediately upon appearance of purple color, detergent solution (100 µL/well) was added and the cells further incubated for 1.5 h at 37 °C. The optical density (OD; λ = 570 nm) was measured (Microplate reader ELx800; BioTek, USA). Non-linear regression analysis was performed (Excel software 2010; Microsoft Corp., USA) to determine the cell proliferation fraction using the following equation:

$$\text{Cell proliferation fraction} = \frac{ODs - ODb}{ODc - ODb}$$

where ODs, ODb and ODc are the absorbance of sample, blank and negative control, respectively. The data were presented as fold-increase in cell proliferation in relation to the untreated control (Al-Said et al., 2017).

2.5. Molecular docking studies

Interaction of the isolated compounds **(SMC 1–5)** with cell signaling molecules like PTEN and p53 was determined by performing molecular docking with the help of different modules of Schrodinger suite (Schrodinger, LLC, NY, USA) as described previously (AlAjmi et al., 2018). Briefly, the two-dimensional structures of all the compounds were drawn in 2D sketcher and prepared for docking in LigPrep (LigPrep, Schrodinger, LLC, NY, USA) by generating different ionization states of each ligand at pH 7.0 ± 2.0 with the help of Epik-module (Epik, Schrodinger 2018, LCC, NY, USA) followed by desaltation. Further, a maximum of 32 stereoisomers for each ligand was generated and the energy of each stereoisomer was minimized using OPLS3e forefield. The 3D coordinates of PTEN and p53 core domain were retrieved from RCSB database available at https://www.rcsb.org/ with the PDB IDs 5BZX (2.50 Å resolution) and 4HJE (1.91 Å resolution) respectively **(**Chen et al., 2013; Lee et al., 2015**)**. Protein structures were processed and optimized for docking after removing heterogeneous molecules such as water and any bound ligand molecule using protein preparation wizard of Glide (Glide, Schrodinger, LLC, NY, USA). Moreover, missing hydrogen atoms were added, proper bond orders were assigned, zero bond order was assigned to disulfide bonds. Prime (Prime, Schrodinger, LLC, NY, USA) was employed to add any missing side chains and/or missing loops before optimizing the protein for hydrogen-bond network. Finally, energy of the protein was minimized using OPLS3e forecefield. The grid box of 56 × 56 × 56 Å dimensions was generated for PTEN core domain by selecting the bound ligand (tartaric acid) as the centroid of the grid box. and the Solis and Wets local search methods were employed to perform molecular docking. For p53, SiteMap (SiteMap, Schrodinger, LLC, NY, USA) was employed to identify the most probable binding site(s) of p53. A total number of three binding sites (I-III) have been identified for p53. The grid box was generated by selecting the residues of the respective binding sites as the centroid of the corresponding grid boxes with a dimension of 64 × 64 × 64 Å, 64 × 64 × 64 Å, and 56 × 56 × 56 Å for binding sites I, II and III respectively. The binding affinity (K_d) was calculated from Gibb's free energy (ΔG) using the following relation (AlAjmi et al., 2018).

$$\Delta G = -RT\ln K_d$$

where, R (=1.987 cal/mol/K) is the universal gas constant, and T is the temperature (=298 K).

3. Results and discussion

3.1. Isolation and structure elucidation of SMC-1, -2, -3, -4 and -5

Five compounds of diverse nature have been isolated (Fig. 1) from *Suaeda monoica* and were coded as **SMC-1**, **SMC-2**, **SMC-3**, **SMC-4** and **SMC-5**. **SMC-1** showed IR absorption bands for hydroxyl group (3360 cm^{-1}), ester function (1737 cm^{-1}) and aromatic ring (1614, 1519, 1064 cm^{-1}). The EIMS spectrum showed a molecular ion peak at m/z 328 that was consisting with a molecular formula of $C_{21}H_{28}O_3$. The ion fragments arising at m/z 285 [$C_{6'}$ - $C_{7'}$ fission, $C_{18}H_{21}O_3]^+$, 155 [CO-O fission, $C_{11}H_7O]^+$, 173 [M − 155, $C_{10}H_{21}O_2]^+$, 157 [O-CH_2 fission, $C_{10}H_{21}O]^+$, 141 [157 – $CH_4]^+$ and 123 [141 - $H_2O]^+$ indicated that a hydroxyl geranilane-type

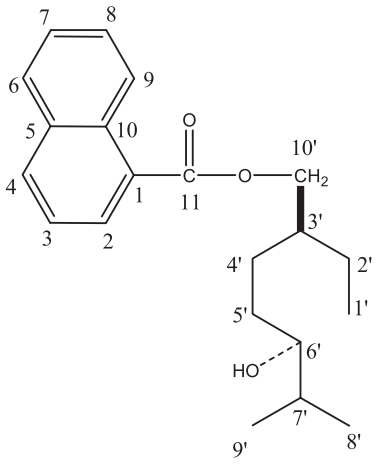

SMC-1

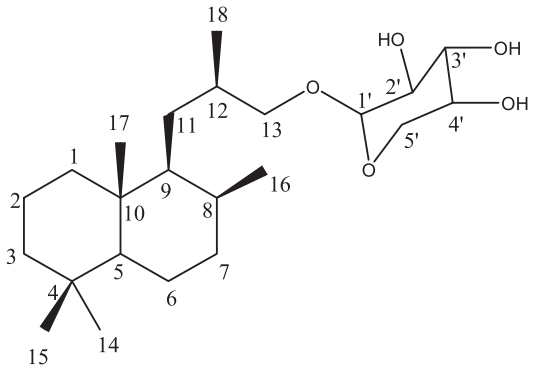

SMC-2

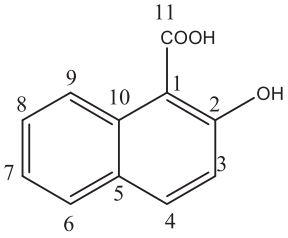

SMC-3

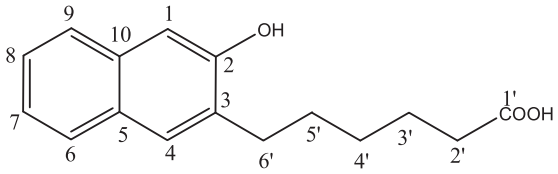

SMC-4

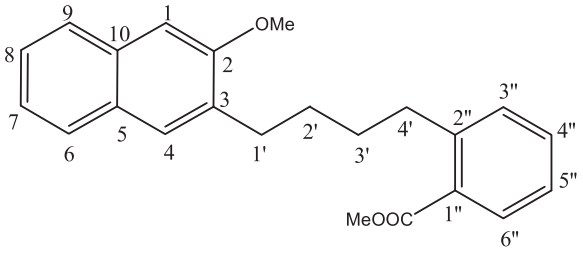

SMC-5

Fig. 1. Chemical structures of compounds (SMC- 1, 2, 3, 4, & 5) isolated from *S. monoica*.

monoterpene moiety could be esterified with naphthoic acid (Fig. 2). The ^{1}H NMR spectrum of **SMC-1** displayed five one proton and a two- proton multiplets from δ 6.62 to 6.38 assigned to naphthyl protons. Two one proton doublets at δ 4.01 (J = 7.5 Hz) and 3.95 (J = 7.0 Hz) were assigned to oxymethylene H_2-10′ protons. One proton multiplet at δ 3.52 with half width of 7.5 Hz was accounted to β-oriented carbinol H-6′ proton. Two three proton doublets at δ 1.25 (J = 6.5 Hz) and 1.23 (J = 6.3 Hz) and a three proton triplet at δ 0.84 (J = 6.5 Hz) were associated with the secondary C-8′ and C-9′ and primary C-1′ methyl protons, respectively. The remaining methylene and methine protons resonated at δ 2.63 to 1.38. The ^{13}C NMR spectrum of **SMC-1** exhibited signals for ester carbon at δ 169.13 (C-11), aromatic carbons in the range of δ 132.63–116.32, oxymethylene carbon at δ 64.62 (C-10′), carbinol carbon at δ 70.10 (C-6′), methyl carbons at δ 9.65 (C-1′), 20.85 (C-8′) and 21.13 (C-9′), and methylene and methine carbons between δ 49.21–22.42. The DEPT spectrum of **SMC-1** showed the presence of three methyl, four methylene and ten methine carbons. The ^{1}H–^{1}H COSY spectrum of **SMC-1** exhibited correlations of H-2 with H-3 and H-4; H-7 with H-6, H-8 and H-9; H-3′ with H_2-2′, H_2-4′, and H_2-10′; and H-7′ with H-6′, Me-8′ and H-9′. The HMBC spectrum of **SMC-1** showed interactions of H-2, H-3 and H-9 with C-1; H-4, H-6 and H-7 with C-5; H-8 and H-9 with C-10; H_2-10′ with C-11; Me-8′, Me-9′ and H-6′ with C-7′; and Me-1′, H_2-2′ and H_2-4′ with C-3′ (Fig. 5**A**). The HSQC spectrum of **SMC-1** exhibited correlation of ^{1}H NMR signals of H_2-10′ at δ 4.01 and 3.95 with

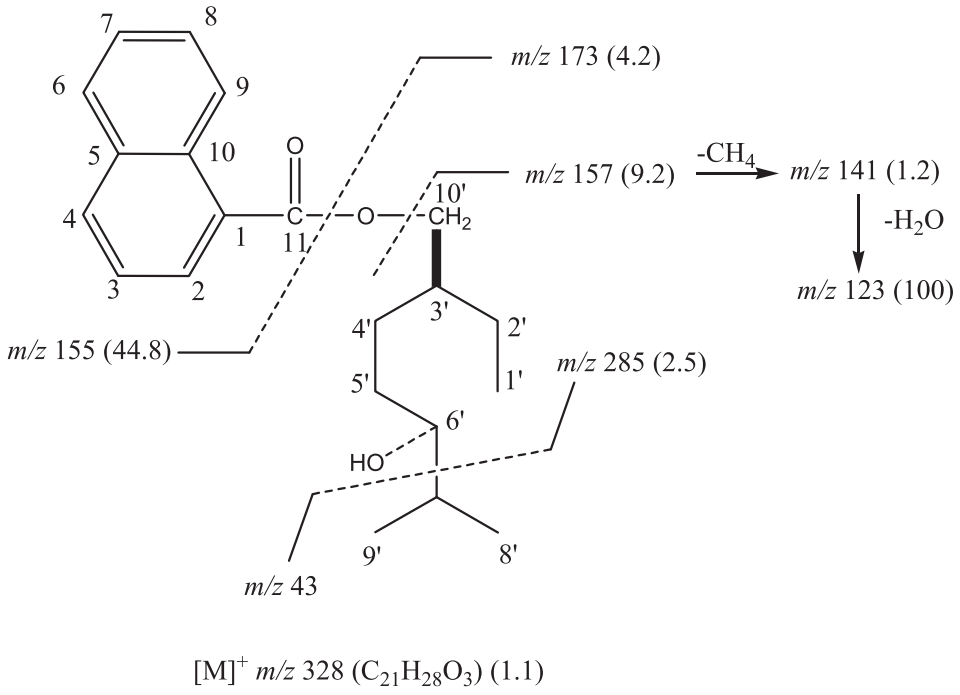

Fig. 2. Mass fragmentation pattern of SMC-1.

carbon signal at δ 64.62 (C-10′); H-6′ ^{1}H NMR signal at δ 3.52 with carbon signal at δ 70.10 (C-6′), methyl proton signals at δ 1.25 (Me-8′), 1.23 (Me-9′) and 0.84 (Me-1′) with their respective carbons at δ 20.85 (C-8′), 21.13 (C-9′) and 9.65 (C-1′), and aromatic proton ^{1}H NMR signal with their corresponding carbon signals. The ^{1}H and ^{13}C NMR spectral data of the naphthyl unit were compared with the reported values of the naphthylene moieties (Aslam et al., 2012; Ali et al., 2014). The spectral data of the geranilany units were compared with the published data of acyclic monoterpenes (Ali, 2001). On the basis of these spectral data analysis the structure of **SMC-1** has been elucidated as 6′-hydroxy-10′-geranilanyl 1-naphthoate, a new aromatic monoterpenic ester.

SMC-2 gave positive test of glycosides and showed IR absorption bands for hydroxyl group (3415, 3392 cm^{-1}). Its molecular ion peak was determined at *m/z* 398 in the EIMS spectrum that was consistent with a molecular formula of a labdane-type norditerpenic glycoside $C_{23}H_{42}O_5$. The ion peaks arising at *m/z* 133 [$C_{1'}$-O fission, $C_5H_9O_4]^+$, and 149 [C_{13}-O fission, $C_5H_9O_5]^+$ suggested the presence of a pentose sugar in the molecule. The ion fragments generated at *m/z* 383 [M−Me]$^+$, 368 [M−2xMe]$^+$, 234 [383–149]$^+$, 163 [C_{12}-C_{13} fission, $C_5H_9O_5$-$CH_2]^+$, 205 [C_9-C_{11} fission, $C_5H_9O_5$-CH_2-CH-(Me)-$CH_2]^+$ supported nor diterpenic nature of the molecule (Fig. 3**).** The ^{1}H NMR spectrum of **SMC-2** exhibited a one- proton doublet at δ 4.23 (J = 7.5 Hz) assigned to the anomeric H-1′ proton. Two one proton double doublets at δ 3.51 (J = 6.2 Hz, 1.1 Hz) and 3.42 (J = 6.3 Hz, 1.1 Hz) were ascribed to oxymethylene H_2-13 protons. Two one-proton double doublets at δ 3.09 (J = 7.1, 1.2 Hz) and 3.06 (J = 6.9, 1.2 Hz) were due to oxymethylene H_2-5′ protons. Three one-proton multiplets at δ 3.40, 3.23 and 3.02 were accounted to sugar carbinol H-4′, H-2′ and H-3′ protons, respectively. Two doublets at δ 0.76 (J = 6.1 Hz) and 0.73 (J = 6.5 Hz) and three singlets at δ 0.90, 0.82 and 0.65, all integrated for three protons each, were accounted to secondary C-18 and C-16, and tertiary C-17, C-15 and C-14 methyl protons, respectively, all attached to saturated carbons. The remaining methylene and methine protons resonated between δ 2.89–1.14. The ^{13}C NMR spectrum of **SMC-2** displayed signals for anomeric carbon at δ 101.25 (C-1′), other sugar carbons from δ 76.71 to 66.15, oxymethylene carbon at δ 61.04 (C-13), methyl carbons at δ 11.74 (C-14), 18.90 (C-15), 19.06 (C-16), 19.68 (C-17), and 18.58 (C-18), and the remaining methine and methylene carbons in the range of δ 57.18–25.48. The absence of any ^{1}H NMR signal beyond δ 4.23 and ^{13}C NMR signal after δ 101.25 supported saturated nature of the molecule. The DEPT spectrum of **SMC-2** showed the presence of five methyl and eight each of methylene and methine carbons. The ^{1}H–^{1}H COSY spectrum of **SMC-2** exhibited correlations of H-1′ with H-2′, H-3′ with H-4′; H-5 with H_2-6, H_2-6 with H_2-7, and H-9 with H-8 and H_2-11. The HMBC spectrum of **SMC-2** showed correlations of H_2-13, H-3′ and H-2′ with C-1′; H_2-11, H-13 and Me-18 with C-12; H-3′ and H_2-5′ with C-4′; H_2-1, Me-17, H_2-11 and H-9 with C-10; and H_2-3, H-5, Me-14 and Me-15 with C-4 (Fig. 5**B**). The HSQC spectrum of **SMC-2** displayed interactions of ^{1}H NMR signals at δ 3.51 and 3.42 (H_2-13) with ^{13}C NMR at δ 61.04 (C-13), anomeric ^{1}H NMR signal at δ 4.23 (H-1′) with the carbon signal at δ 101.25 (C-1′) and the methyl protons signals with the respective carbon signals. The ^{1}H and ^{13}C NMR data of diterpenic nucleus of **SMC-2** were compared with the reported values of the labdane-type and related compounds and it was concluded that the molecule was a norlabdanoyl glycoside possessing two less carbon atoms in the side chain (Ali, 2001; Al-Massarani et al, 2017; Zheng et al., 2012; Demetzos and Dimas, 2001; Sy and Brown, 1997). Acid hydrolysis of **SMC-2** yielded norlabdan-13-ol and D-xylose, R_f 0.76 (*n*-butanol: acetic acid: water, 4:1:1.6). On the basis of foregoing discussion, the structure of compound **SMC–2** has been characterized as 4,4,8β,10β-Tetramethyl-9β-isobutanyl-13-ol-13-β-D-xylopyranoside, an unknown labdane-type nor diterpene xyloside.

SMC-4 produced effervescences with sodium bicarbonate solution and showed IR absorption bands for hydroxyl group (3407 cm^{-1}), carboxyl function (3209, 1677 cm^{-1}) and aromatic ring (1521, 1108 cm^{-1}) and aliphatic chain (775 cm^{-1}). Its molecular ion peak was determined at *m/z* 258 on the basis of mass and ^{13}C NMR spectra corresponding to molecular formula of alkylated naphthol. The ^{1}H NMR spectrum of **SMC-4** exhibited two one- proton singlets assigned to p-coupled aromatic H-1 and H-4 protons, respectively. Other aromatic protons as a one- proton double

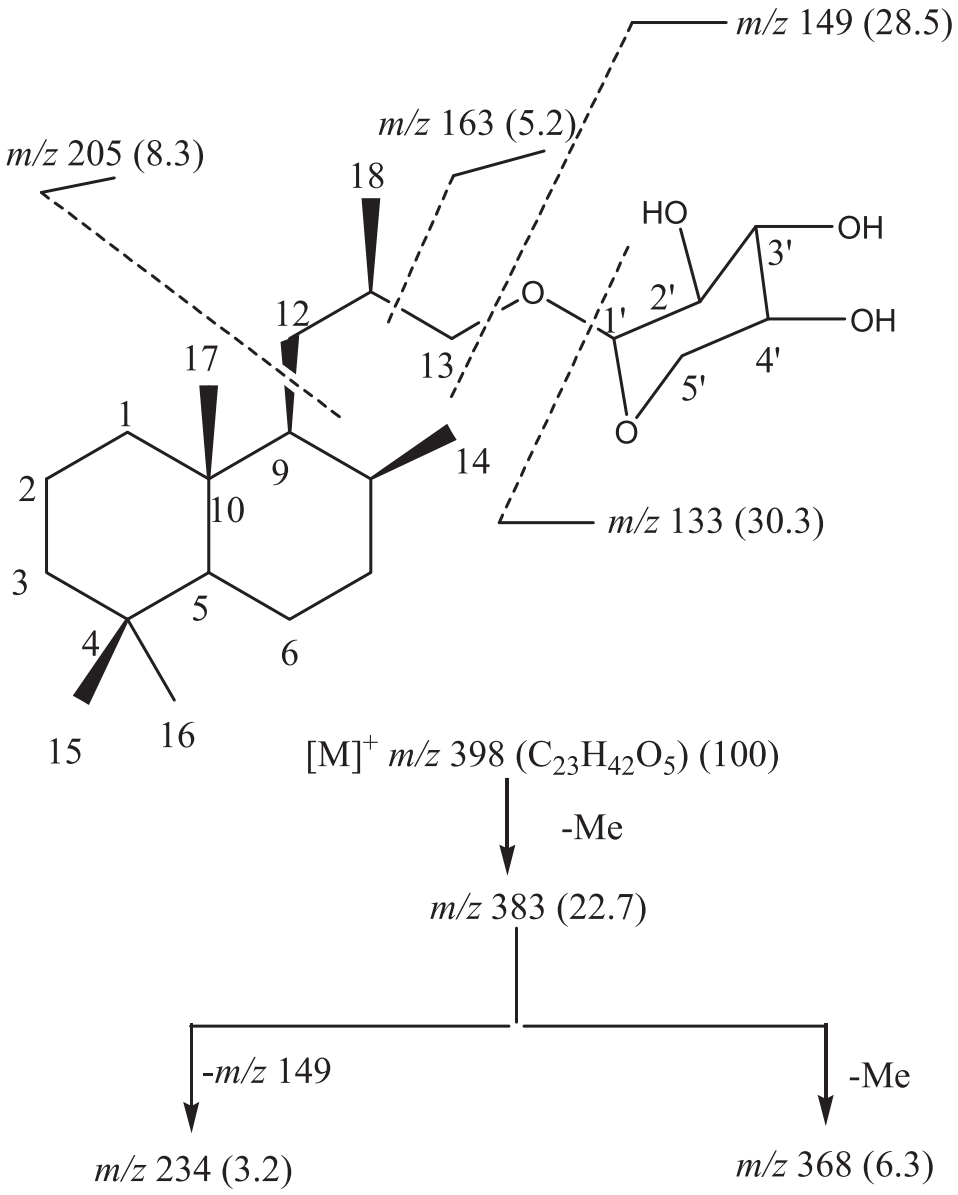

Fig. 3. Mass fragmentation pattern of SMC-2.

doublet at δ 6.95 (J = 2.0, 7.3 Hz, H-9), as a one- proton doublet at δ 6.69 (J = 8.0 Hz, H-6), and as one- proton multiplets at δ 6.45 (H-8) and 6.02 (H-7). Two two- proton triplets at δ 4.43 (J = 7.5 Hz) and 2.86 (J = 7.5 Hz), and three two- proton multiplets at δ 2.29, 1.58 and 1.27 were ascribed to methylene H_2-6′ attached to the aromatic ring and methylene H_2-2′ adjacent to the carboxyl function and the other methylene H_2-5′, H_2-4′ and H_2-3′ of the side chain. The ^{13}C NMR spectrum of **SMC-4** displayed signals for carboxylic carbon at δ 178.37 (C-1′), aromatic carbons between δ 164.56–117.02 and methylene carbons from δ 52.10 to 26.04. The DEPT spectrum of **SMC-4** showed the presence of five methylene and six methine carbons. The ^{1}H–^{1}H COSY spectrum of **SMC-4** exhibited correlations of H-7 with H-6, H-8 and H-9; H-4 with H_2-6′, and H_2-2′ with H_2-3′ and H_2-4′. The HMBC spectrum of **SMC-4** showed interactions of H-1 and H-9 with C-10; H-4 and H_2-6′ with C-3; H-1 and H-4 with C-2; H-4 and; H-6 and H-7 with C-5; and H_2-2′ with C-1′ (Fig. 5**C**). The HSQC spectrum of **SMC-4** displayed correlation of ^{1}H NMR signals at δ 6.73 (H-1), 6.60 (H-4), 6.95 (H-9) and 6.69 (H-6) with their respective aromatic carbon signals at δ 124.80 (C-1), 127.10 (C-4), 127.82 (C-9) and 120.62 (C-6); and methylene proton signals at δ 2.86 (H_2-6′) and 2.42 (H_2– 2′) with the carbon signals at δ 52.10 (C-6′) and 38.66 (C-2′). On the basis of these evidences, the structure of **SMC-4** was elucidated as 6-(2 -hydroxynaphthalen-3-yl)hexanoic acid; a new alkylated β-naphthol.

SMC-5 had IR absorption bands for ester group (1733 cm^{-1}) and aromatic rings (1637, 1596, 1515, 1031 cm^{-1}). On the basis of mass and ^{13}C NMR spectra the molecular ion peak of **SMC-5** was established at m/z 348 corresponding to a molecular formula of a naphthyl benzoyl butane derivative, $C_{23}H_{24}O_3$. The ion peaks arising at m/z 135 [$C_{4'}$-$C_{2''}$ fission, C_6H_4-COOMe]$^+$, 105 [135-OMe]$^+$ and 77 [135-COOMe]$^+$ indicated that methyl benzoate group was present in the molecule. The ion fragments generated at m/z 149 [$C_{3'}$-$C_{4'}$ fission, CH_2-C_6H_4-COOMe]$^+$ [M−Me]$^+$, 163 [$C_{2'}$-$C_{3'}$ fission, CH_2-CH_2-C_6H_4-COOMe]$^+$, 177 [$C_{1'}$-$C_{2'}$ fission, $(CH_2)_3$-C_6H_4-COOMe]$^+$ and 191 [C_3-C_1 fission, $(CH_2)_4$-C_6H_4-COOMe]$^+$ suggested that methyl benzoate was attached to one of the end of n-butane and methoxy (Fig. 4). Naphthalene was linked to another end carbon of n-butane chain. The ^{1}H NMR spectrum of **SMC-5** exhibited four one- proton double doublets at δ 7.46 (J = 10.5, 2.3 Hz), 7.06 (J = 9.0,

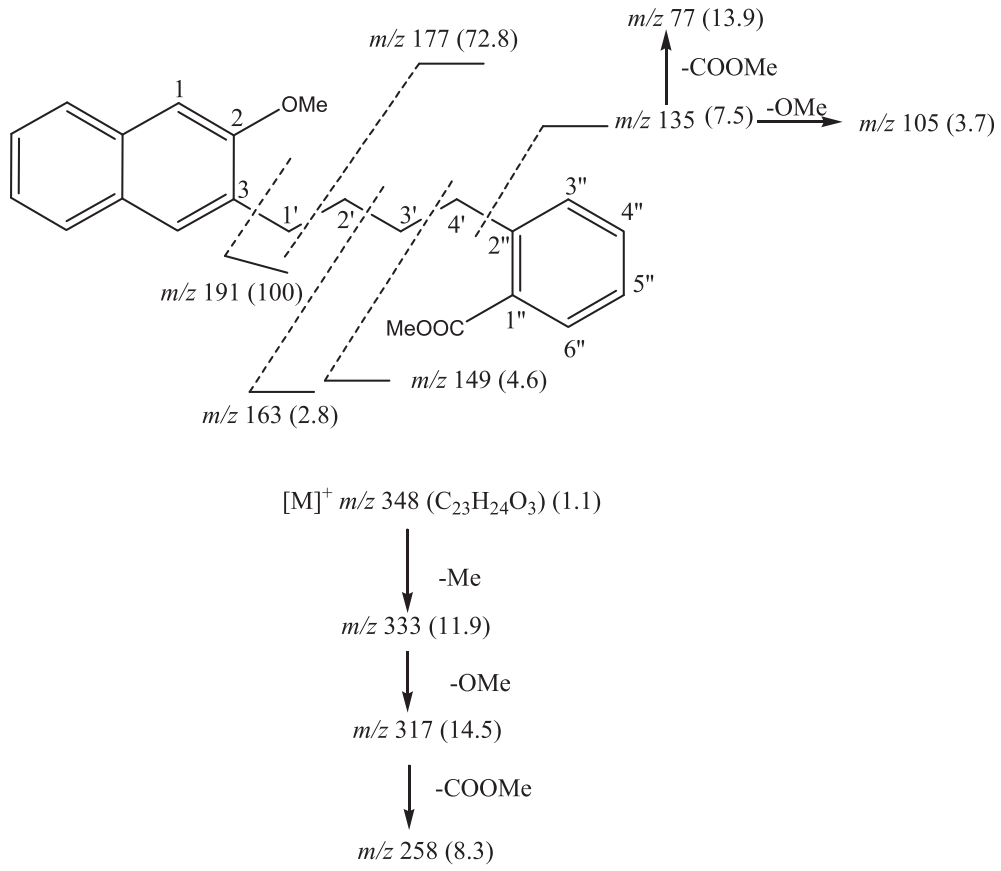

Fig. 4. Mass fragmentation pattern of SMC-5.

1.0 Hz), 7.04 (J = 8.5, 1.0 Hz) and 6.82 (J = 8.1, 1.5 Hz) were assigned to ortho-, meta- coupled aromatic H-6′′, H-3′′, H-6 and H-9 protons, respectively. Two one proton singlets at δ 7.12 and 6.41, and two three-proton singlets at δ 3.85 and 3.37 were attributed correspondingly to p-coupled H-1 and H-4 and to methoxy protons. The other aromatic protons resonated as two proton multiplets at δ 6.75 (H-7, H-4′′) and 6.45 (H-5′and H-8). Two triplets at δ 3.46 (J = 7.5 Hz) and 3.33 (J = 1.5 Hz) and two-multiplets at δ 2.78 and δ 1.26, all integrating for two-protons each, were associated with the methylene H_2-1′, H-4′, H-3′ and H-2′ protons, respectively. The ^{13}C NMR spectrum of **SMC-5** displayed carbon signals for ester carbon at δ 169.47 (C-7′′), aromatic carbons between δ 156.61 to 116.41, methoxy carbons at δ 56.57, 50.01 and methylene carbons from δ 49.67 to 35.73. The DEPT spectrum of **SMC-5** showed the presence of two methoxy, four methylene and ten methine carbons. The ^{1}H–^{1}H COSY spectrum of **SMC-5** exhibited correlations of H-4′′ with H-3′′ and H-5′′; H-5′′ with H-6′′; H-7 with H-6 and H-8; H-8 with H-9; H-4′′ with H-3′′; and H-3′ with H_2-4′ and H_2-2′. The HMBC spectrum of **SMC-5** displayed interactions of H-4, H-1 and H_2-1′ with C-3; H-1, H-8 and H-9 with C-10; H-4, H-6 and H-7 with C-5; H_2-4′ and H-3′′ with C-2′′; and H-6′′ and H-5′′ with C-1′′ (Fig. 5D). The HSQC spectrum of **SMC-5** showed correlations of ^{1}H NMR signals at δ 7.12 (H-1), 6.41 (H-4) and 3.46 (H_2-1′) with the respective carbon signals at δ 123.43 (C-1), 128.01 (C-4) and 49.67 (C-1′); ^{1}H NMR signals at δ 7.04 (H-3′′), 7.46 (H-6′′) and 3.33 (H_2-4′), with the carbon signals at δ 128.37 (C-3′′), 132.19 (C-6′′) and 42.71 (C-4′), respectively. On the basis of these evidences the structure of **SMC-5** has been established as 1′-(2-Methoxy-3-naphthyl)-4′-(2′′-methylbenzoyl)-n-butane, a new β-methoxy-naphthalene derivative.

SMC-3 gave effervescence with sodium bicarbonate solution and showed IR absorption bands for hydroxyl group (3477 cm^{-1}), carboxylic function (1670 cm^{-1}) and aromatic ring (1600, 1512, 977 cm^{-1}). Its molecular ion peak was determined at m/z 188 on the basis of mass and ^{13}C NMR spectra consistent with the molecular formula of hydroxyl aromatic acid, $C_{11}H_8O_3$. The ^{1}H NMR spectrum of **SMC-3** exhibited four one- proton doublets at δ 7.59 (J = 16.0 Hz), 7.44 (J = 9.0 Hz), 7.42 (J = 9.0 Hz) and 6.30 (J = 16.0 Hz) assigned to *ortho*-coupled H-3, H-6, H-9 and H-4 and two one-proton multiplets at δ 6.84 and 6.82 accounted to H-7 and H-8 protons, respectively. The ^{13}C NMR spectrum of **SMC-3** displayed the presence of eleven carbon attributed to carboxylic carbon at δ 171.49 (C-11) and hydroxyl naphthalene carbons from δ 160.93 to 115.56. The DEPT spectrum of **SMC-3** showed six methine carbon signals. Its ^{1}H–^{1}H COSY spectrum displayed correlations of H-3 with H-4; and H-7 with H-6, and H-8; and H-8 with H-9. The HMBC spectrum of **SMC-3** exhibited interactions of H-3 and H-4 with C-2 and C-5; H-6 with C-5, and H-8 with C-10. The HSQC spectrum showed that ^{1}H NMR signals at δ 7.59 (H-3) and 6.30 (H-4) correlated with carbon signals at δ 131.85 (C-3) and 131.21 (C-4), respectively, and proton signals at δ 7.44 (H-6), 7.42 (H-9), 6.84 (H-7) and 6.82 (H-8) with their corresponding carbon signals at δ 127.33 (C-6), 127.53 (C-9), 115.56 (C-7) and 116.26 (C-8). The chemical structure of SMC-3 has been confirmed from the spectral data of previous research work reported by Elsayed et al., 2013.On the basis of above discussion, the structure of **SMC-3** has been elucidated as 2-Hydroxy-1-naphthoic acid. The acid is utilized by *Burkholderia* species strain BC1 as the sole source of carbon and energy (Chowdhury et al., 2014).

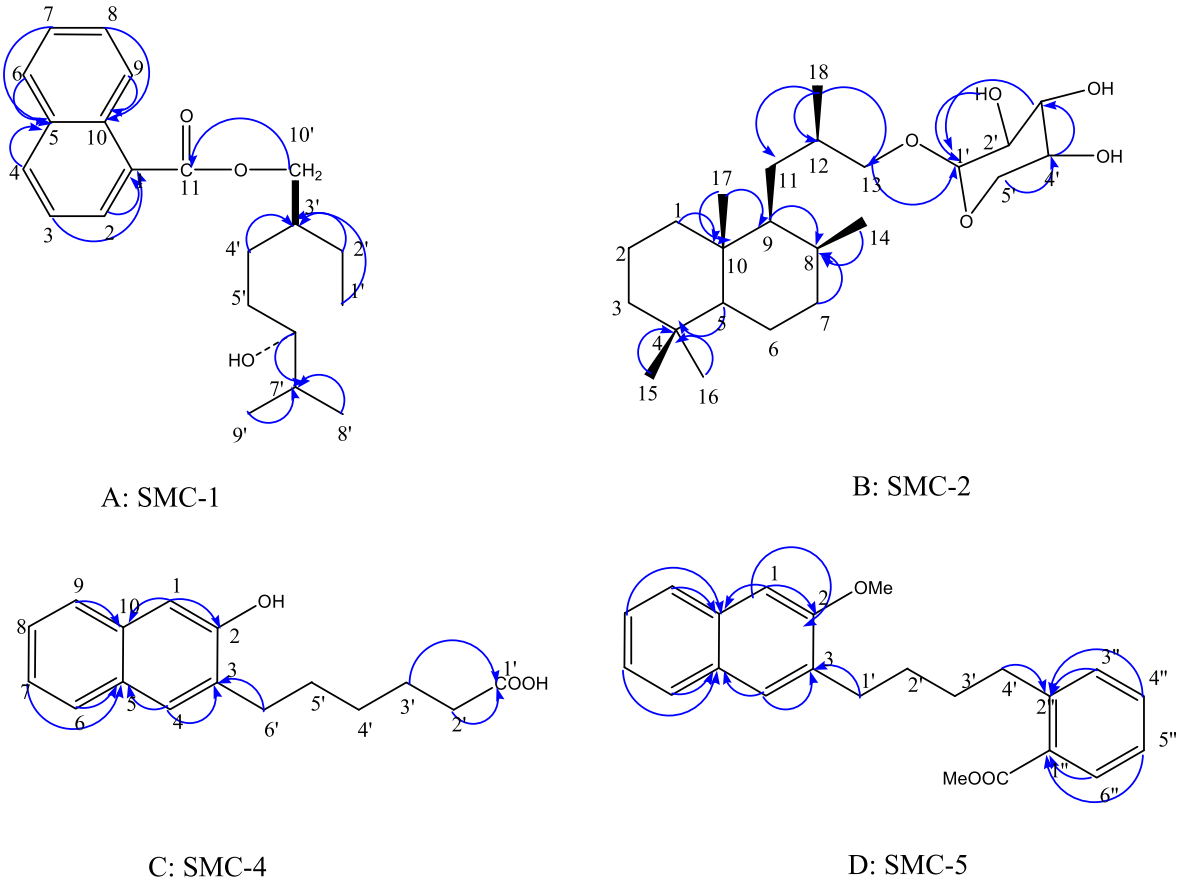

Fig. 5. HMBC correlations of SMC compounds.

3.2. Cell proliferative potential of SMC compounds

All five compounds were found to be nontoxic towards HepG2 cells (data not shown). Notably, the final concentration of DMSO was < 0.1% in the highest tested dose (50 μg/mL) where the cell viability was comparable to the untreated control. Therefore, the compounds were further evaluated for cell proliferative activities at the 50 μg/mL dose. The MTT assay showed the marked cell proliferative potential of all five compounds (1.42–1.48 fold) as compared to untreated control (Fig. 6).

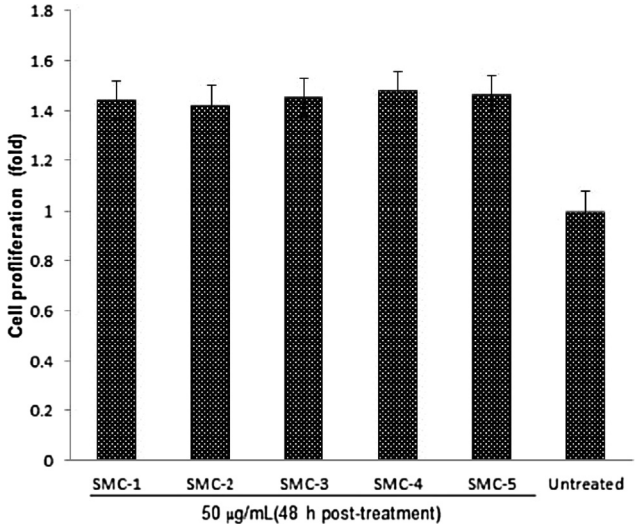

Fig. 6. The HepG2 cell proliferative potential of the five isolated compounds from *S. monoica*.

Many herbs have shown the cell proliferation potential, which is considered as one of the most useful methods for tissue regeneration, repair and aging. Blue berry, green tea, catechin, carnosine, and vitamin D3 were proved to have cell proliferation potential on human bone marrow as compared with human granulocyte macrophage colony-stimulating factor (h GM-CSF). Further studies showed that an interaction of nutrients with stem cell populations can promote rejuvenation (Bickford et al., 2006). There are several other natural compounds such as betulin and betulinic acid, which had previously been reported for cell proliferative potential and exhibited mitogenic activity with the ability to induce and modulate cytokine production in human blood leucocyte cells (Zdzisińska et al., 2003). It is observed that cell proliferation rate of mouse bone marrow mesenchymal stem cells enhanced up to 122.24% compared to untreated cells when treated with roots of *Aconiti lateralis* (Kim et al., 2013). The findings of this experiment, which showed 1.42- to 1.48-fold increase in cell proliferation as compared to untreated cells may pave a way to explore the removal of blockade on check points or stimulation of immunotherapeutic channels to treat some dreaded diseases.

3.3. Molecular docking analysis: Interaction of SMC compounds with cell signaling molecules (PTEN and p53)

3.3.1. Interaction between SMC compounds and PTEN

PTEN (phosphatase and tensin homologue deleted on chromosome 10) is a PI (phosphoinositide) 3-phosphatase. It acts as a tumor suppressor protein by inhibiting cellular proliferation, survival, and growth by inactivating PI3K-dependent signaling

pathways. It antagonizes PI3K signaling pathway by dephosphorylating phosphatidylinositol 3,4,5-triphosphate into phosphatidylinositol 4,5-diphosphate (Leslie and Downes, 2004). In most of the cases where uncontrolled cell proliferation occurs, PTEN has been found to be inhibited or inactivated by different mutations. Thus, it is interesting to see whether the SMC compounds isolated in this study promote cell proliferation by inhibiting or inactivating PTEN. For this purpose, we employed molecular docking to gain an insight into the mechanism by which SMC compounds bind to PTEN. It is clear from Fig. 7**A** that all the SMC molecules (1–5) were bound at the same site.

SMC-1 interacted with PTEN by forming one hydrophobic interaction with His93 in addition to three hydrogen bonds with Asp92, Gly129 and Tyr176 **(**Fig. 7**B)**. Moreover, a cation-Pi interaction was observed between SMC-1 and Lys128. Other amino acid residues involved in the interaction were Val45, Arg47, Cys124, Lys125, Ala126, Gly127, Ile168, Gln171, Arg130, Thr131, and Lys330. The Gibb's free energy of binding was estimated to be −6.660 kcal/mol, corresponding to a binding affinity of 7.67×10^4 M^{-1} **(**Table 1**)**.

The PTEN-**SMC-2** complex was stabilized by five hydrogen bonds with Asp92, Ala126, Lys128, Arg130, Thr131 **(**Table 1**)**. Moreover, Arg47, His93, Cys124, Lys125, Gly127, Gly129, Gly132, Gln171, and Lys330 of PTEN were also involved in the stability of PTEN-SMC-2 complex (Fig. 7**C**). The PTEN-SMC-2 complex was stabilized by −6.564 kcal/mol of free energy, which is corresponded to a binding affinity of 6.52×10^4 M^{-1} **(**Table 1**)**.

The complex between **SMC-3** and PTEN was stabilized by one cation-Pi interaction with Arg47 and four hydrogen bonds with Asp92, Lys125, Gly127, and Thr131 (Fig. 7**D**). Other amino acid residues involved in the interaction between SMC-3 and PTEN were His93, Cys124, Ala126, Lys128, Gly129, and Arg130 **(**Fig. 7**D).** The binding free energy and binding affinity of PTEN-SMC-3 complex formation were – 7.149 kcal/mol, and 1.75×10^5 M^{-1}, respectively **(**Table 1**).**

SMC-4 formed one hydrophobic interaction with His93 and two cation-Pi interactions with Lys128 and Arg161 of PTEN. Other amino acid residues involved in PTEN-SMC-4 complex formation were Tyr16, Asp92, Cys124, Lys125, Ala126, Gly127, Gly129, Arg130, Thr131, Arg159, Thr160, Asp162, and Lys164 (Fig. 7**E**). Gibb's free energy of the interaction between SMC-4 and PTEN was estimated to be −6.748 kcal/mol while the binding affinity was determined to be 8.89×10^4 M^{-1} (Table 1).

Similarly, **SMC-5** interacted with PTEN by forming two hydrophobic interactions with His93 and two hydrogen bonds with Ala126 and Gln171 (Table 1). Moreover, Arg130 formed a salt bridge with PTEN. Several other residues such as Arg47, Asp92, Cys124, Lys125, Gly127, Lys128, Gly129, and Ile168 were also involved in the formation of a stable complex between SMC-5 and PTEN (Fig. 7**F**). Gibb's free energy of stabilization and binding affinity of SMC-5 towards PTEN were estimated to be −7.321 kcal/mol, and 2.34×10^5 M^{-1}, respectively (Table 1).

The results of molecular docking could be better interpreted after gaining an insight into the three-dimensional structure of PTEN. It is a 403 amino acid long protein composed of two major domains namely N-terminal phosphatase domain (residues 7–185), and C-terminal C2 domain (residues 186–351). The active site of PTEN is made up of residues 123–130 with a signature HCXXGXXR motif (Leslie and Downes, 2004). In addition, Asp92 acts as a general acid to facilitate protonation of the O-atom of the tyrosyl leaving group. Several other residues such as residues 42–52, residues 91–94, residues 163–166, and Gln171 play significant role in the recognition of the substrate and its hydrolysis (Lee et al., 1999). From our docking results, we observed that the SMC compounds **(SMC 1–5)** bind at the active site of and thus may sterically hinder the accessibility of phosphatidylinositol 3,4,5-triphosphate to the active site thereby preventing the dephosphorylation of phosphatidylinositol 3,4,5-triphosphate by PTEN. The intact phosphatidylinositol 3,4,5-triphosphate molecule will then be available for PI3K signaling pathway and other downstream pathways involved in the cellular growth and survival.

3.3.2. Interaction between SMC compounds and p53

p53 is a tumor suppressor protein which subdues tumor formation and progression by regulating various transcriptional pathways involved in cell cycle arrest, DNA repair, and apoptosis (Bai and Zhu, 2006). p53 is a tetrameric phosphoprotein comprising 393 amino acids organized into well-structured domains as well as unstructured regions working synergistically. It comprises four domains that perform specific functions such as (i) activation of transcription factors by transactivation domain, (ii) recognition of specific DNA sequences by DNA-binding domain, (iii) tetramerization of the protein by tetramerization domain, and (iv) recognition of damaged DNA by regulatory domain. The loss of p53 tumor suppressor function results in uncontrolled proliferation of cells thereby leading to the formation of cancers. Thus, it is interesting to know whether SMC compounds induce cellular progression by binding to p53 and thus inactivating it.

The most probable binding site(s) on p53 was determined using Epik-module (Epik, Schrodinger 2018, LCC, NY, USA). We found that three binding sites (I-III) were present on p53, relative locations of which are shown in supplementary **Fig. S1**. The analysis of binding site has shown that SMC molecules have relatively higher affinity towards binding sites I and II as compared to binding site III. Thus, the results of binding sites I and II have been discussed here, while the results of binding site III has been reported as supplementary data (**Fig. S1** and **Table S1**). Results representing the nature of interactions and the type of amino acid residues involved in the formation of stable SMC-p53 complex are given in Table 2 and Fig. 8**,9**. The results presented in Fig. 8**A** and Fig. 9**A** confirm that all the SMC molecules (1–5) were bound at the site I and site II, respectively.

3.3.2.1. Interaction of SMC molecules at the binding site I. **SMC-1** interacted with p53 by forming two hydrogen bonds with Cys229 and Thr231 (Fig. 8**B**). Other amino acid residues involved in the interaction were Gln144, Val197, Glu198, Gly199, Asn200, Val218, Pro219, Tyr220, Glu221, Glu224, Ser227, Thr230, Ile232, and His233. The Gibb's free energy of binding was estimated to be −6.186 kcal/mol, corresponding to a binding affinity of 3.44×10^4 M^{-1} (Table 2).

The p53-**SMC-2** complex was stabilized by five hydrogen bonds with Glu198, Gly199, Asn200, and His233 (Fig. 8**C**). Moreover, Val197, Val218, Glu221, Pro222, Pro223, Glu224, Ser227, Cys229, Thr230, Thr231, and Ile232 of p53 formed multiple van der Waals interactions with SMC-2 (Fig. 8**C**). The p53-SMC-2 complex was stabilized by −6.529 kcal/mol of free energy, which is corresponded to a binding affinity of 6.15×10^4 M^{-1} (Table 2).

The complex between **SMC-3** and p53 was stabilized by three hydrogen bonds with Asn200, Pro222 and His233 (Fig. 8**D**). Other amino acid residues involved in the interaction between SMC-3 and p53 were Val197, Glu198, Gly199, Val218, Glu221, Pro223, Glu224, Ser227, Cys229, Thr230, Thr231, and Ile232 (Fig. 8**D**). The binding free energy and binding affinity of p53-SMC-3 complex formation were −6.887 kcal/mol, and 1.12×10^5 M^{-1} respectively (Table 2).

SMC-4 formed one hydrogen bond with Thr231 of p53. Other amino acid residues involved in p53-SMC-4 complex formation were Gln144, Ile145, Val157, Val197, Glu198, Gly199, Asn200, Val218, Pro219, Tyr220, Glu221, Pro223, Glu224, Ser227, Cys229, Thr230, Ile232, and His233 (Fig. 8**E**). Gibb's free energy of the interaction between SMC-4 and p53 was estimated to be

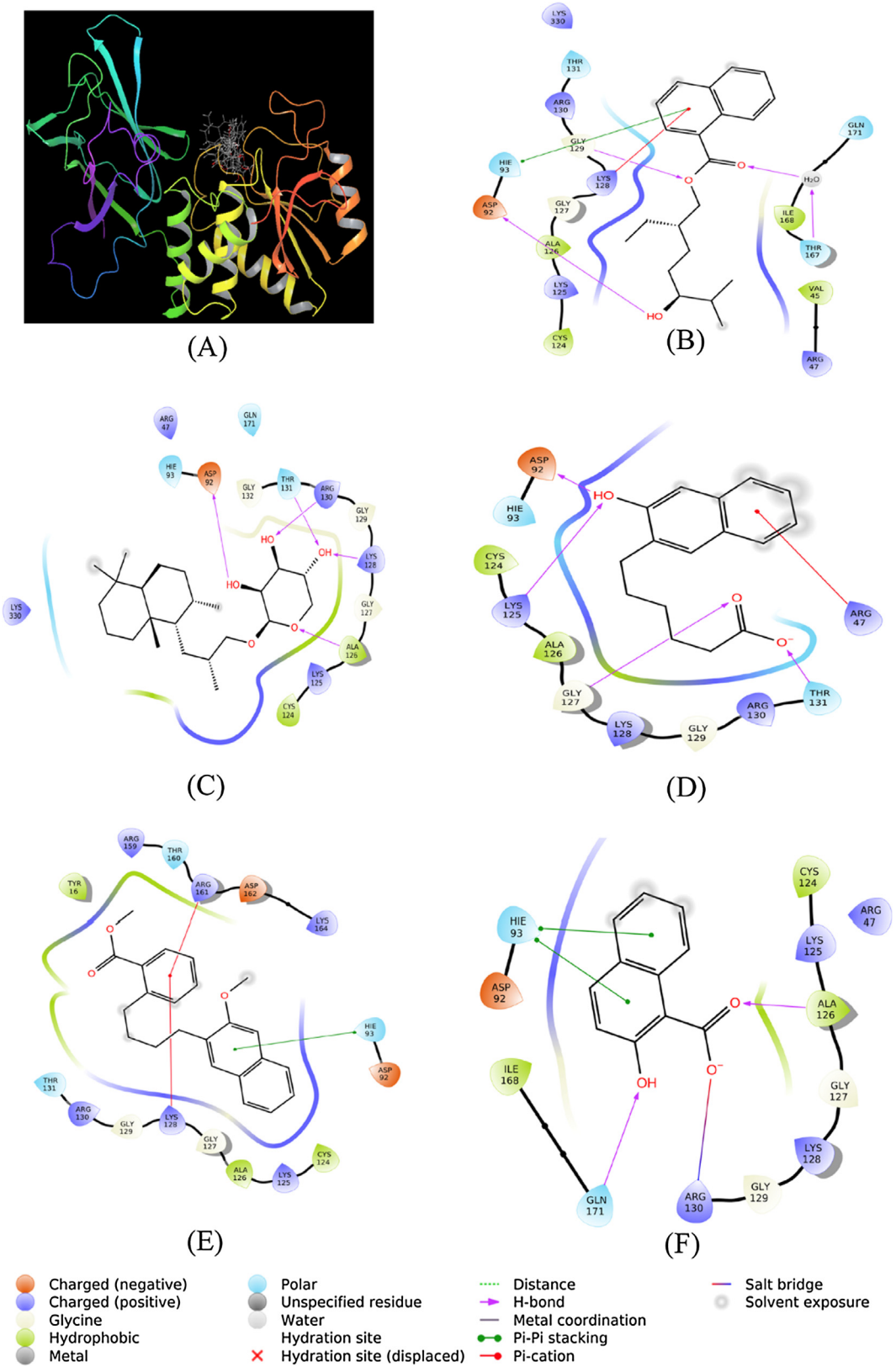

Fig. 7. Binding of SMC compounds with PTEN. Binding of (A) all SMC compounds, (B) SMC-1, (C) SMC-2, (D) SMC-3, (E) SMC-4, (F) SMC-5.

−5.608 kcal/mol while the binding affinity was determined to be $1.29 \times 10^4\ M^{-1}$ (Table 2).

Similarly, **SMC-5** interacted with p53 by forming one hydrogen bond with Glu198 (Table 2). Several other residues such as Val197, Gly199, Asn200, Val218, Pro219, Tyr220, Glu221, Thr230, Thr231, Ile232, and His233 were also involved in the formation of a stable complex between SMC-5 and p53 (Fig. 8**F**). Gibb's free energy of stabilization and binding affinity of SMC-5 towards p53 were

Table 1
Interaction of SMC compounds with PTEN.

Compound ID	Hydrophobic interactions	Hydrogen bonding	Cation-Pi interactions	Other residues involved	Binding energy (ΔG), kcal/mol	Binding affinity, K_d (M^{-1})
SMC-1	His93	Asp92, Gly129, Thr167	Lys128	Val45, Arg47, Cys124, Lys125, Ala126, Gly127, Ile168, Gln171, Arg130, Thr131, Lys330	−6.660	7.67×10^4
SMC-2	–	Asp92, Ala126, Lys128, Arg130, Thr131	–	Arg47, His93, Cys124, Lys125, Gly127, Gly129, Gly132, Gln171, Lys330	−6.564	6.52×10^4
SMC-3	–	Asp92, Lys125, Gly127, Thr131	Arg47	His93, Cys124, Ala126, Lys128, Gly129, Arg130	−7.149	1.75×10^5
SMC-4	His93	–	Lys128, Arg161	Tyr16, Asp92, Cys124, Lys125, Ala126, Gly127, Gly129, Arg130, Thr131, Arg159, Thr160, Asp162, Lys164	−6.748	8.89×10^4
SMC-5	His93[#]	Ala126, Gln171	Arg130[*]	Arg47, Asp92, Cys124, Lys125, Gly127, Lys128, Gly129, Ile168	−7.321	2.34×10^5

[#] Two interactions.
[*] Salt bridge.

Table 2
Interaction of SMC compounds with p53.

Compound ID	Hydrophobic interactions	Hydrogen bonding	Cation-Pi interactions	Other residues involved	Binding energy (ΔG), kcal/mol	Binding affinity, K_d (M^{-1})
Site I						
SMC-1	–	Cys229, Thr231	–	Gln144, Val197, Glu198, Gly199, Asn200, Val218, Pro219, Tyr220, Glu221, Glu224, Ser227, Thr230, Ile232, His233	−6.186	3.44×10^4
SMC-2	–	Glu198, Gly199[#], Asn200, His233	–	Val197, Val218, Glu221, Pro222, Pro223, Glu224, Ser227, Cys229, Thr230, Thr231, Ile232	−6.529	6.15×10^4
SMC-3	–	Asn200, Pro222, His233	–	Val197, Glu198, Gly199, Val218, Glu221, Pro223, Glu224, Ser227, Cys229, Thr230, Thr231, Ile232	−6.887	1.12×10^5
SMC-4	–	Thr231	–	Gln144, Ile145, Val157, Val197, Glu198, Gly199, Asn200, Val218, Pro219, Tyr220, Glu221, Pro223, Glu224, Ser227, Cys229, Thr230, Ile232, His233	−5.608	1.29×10^4
SMC-5	–	Glu198	–	Val197, Gly199, Asn200, Val218, Pro219, Tyr220, Glu221, Thr230, Thr231, Ile232, His233	−5.698	1.51×10^4
Site II						
SMC-1	–	Val97, Ser99	–	Ser96, Pro98, Arg158, Met160, Ile254, Thr256, Glu258, Arg267	−5.106	5.56×10^3
SMC-2	–	Glu258, Gly262[#], Arg267	–	Ser96, Val97, Pro98, Ser99, Leu206, Asp208, Thr211, Arg213, Arg158, Met160, Ile254, Thr256, Asn263, Leu264	−5.598	1.28×10^4
SMC-3	–	Ser99, Glu258	Arg158	Pro98, Met160, Arg213, Thr211, Asp208, Ile254, Thr256, Gly262, Leu264, Arg267	−6.010	2.56×10^4
SMC-4	–	–	–	Ser96, Val97, Pro98, Ser99, Asp208, Arg209, Asn210, Thr211, Arg158, Met160, Ile254, Thr256, Glu258, Leu264, Arg267	−5.711	1.54×10^4
SMC-5	–	Gly262, Arg267	–	Pro98, Ser99, Arg158, Met160, Ile254, Thr256, Glu258, Asn263, Leu264	−5.793	1.77×10^4

[*] Salt bridge.
[#] Two bonds.

estimated to be −5.698 kcal/mol, and 1.51×10^4 M^{-1}, respectively (Table 2).

3.3.2.2. Interaction of SMC molecules at the binding site II. **SMC-1** interacted with p53 by forming two hydrogen bonds with Val97 and Ser99. Other amino acid residues involved in the interaction were Ser96, Pro98, Arg158, Met160, Ile254, Thr256, Glu258, and Arg267 (Fig. 9**B**). The Gibb's free energy of binding was estimated to be −5.106 kcal/mol, corresponding to a binding affinity of 5.56×10^3 M^{-1} (Table 2).

The p53-**SMC-2** complex was stabilized by four hydrogen bonds with Glu258, Gly262 and Arg267 (Fig. 9**C**). Moreover, Ser96, Val97, Pro98, Ser99, Leu206, Asp208, Thr211, Arg213, Arg158, Met160, Ile254, Thr256, Asn263, and Leu264 of p53 formed multiple van der Waals interactions with SMC-2 (Fig. 9**C**). The p53-SMC-2 complex was stabilized by −5.598 kcal/mol of free energy, which is corresponded to a binding affinity of 1.28×10^4 M^{-1} (Table 2).

The complex between **SMC-3** and p53 was stabilized by two hydrogen bonds with Ser99 and Glu258, and one cation-Pi interaction with Arg518 (Fig. 9**D**). Other amino acid residues involved in the interaction between SMC-3 and p53 were Pro98, Met160, Arg213, Thr211, Asp208, Ile254, Thr256, Gly262, Leu264, and Arg267 (Fig. 9**D**). The binding free energy and binding affinity of p53-SMC-3 complex formation were −6.010 kcal/mol, and 2.56×10^4 M^{-1}, respectively (Table 2).

SMC-4 formed did not form any hydrogen bond, hydrophobic or electrostatic interactions with p53 at binding site III. Several amino acid residues such as Ser96, Val97, Pro98, Ser99, Asp208, Arg209, Asn210, Thr211, Arg158, Met160, Ile254, Thr256, Glu258, Leu264, and Arg267 were involved in p53-SMC-4 complex formation (Fig. 9**E**). Gibb's free energy of the interaction between SMC-4 and p53 was estimated to be −5.711 kcal/mol while the binding affinity was determined to be 1.54×10^4 M^{-1} (Table 2).

Similarly, **SMC-5** interacted with p53 by forming two hydrogen bonds with Gly262 and Arg267 (Table 2). Several other residues such as Pro98, Ser99, Arg158, Met160, Ile254, Thr256, Glu258, Asn263, and Leu264 were also involved in the formation of SMC-5-p53 complex (Fig. 9**F**). Gibb's free energy of stabilization and

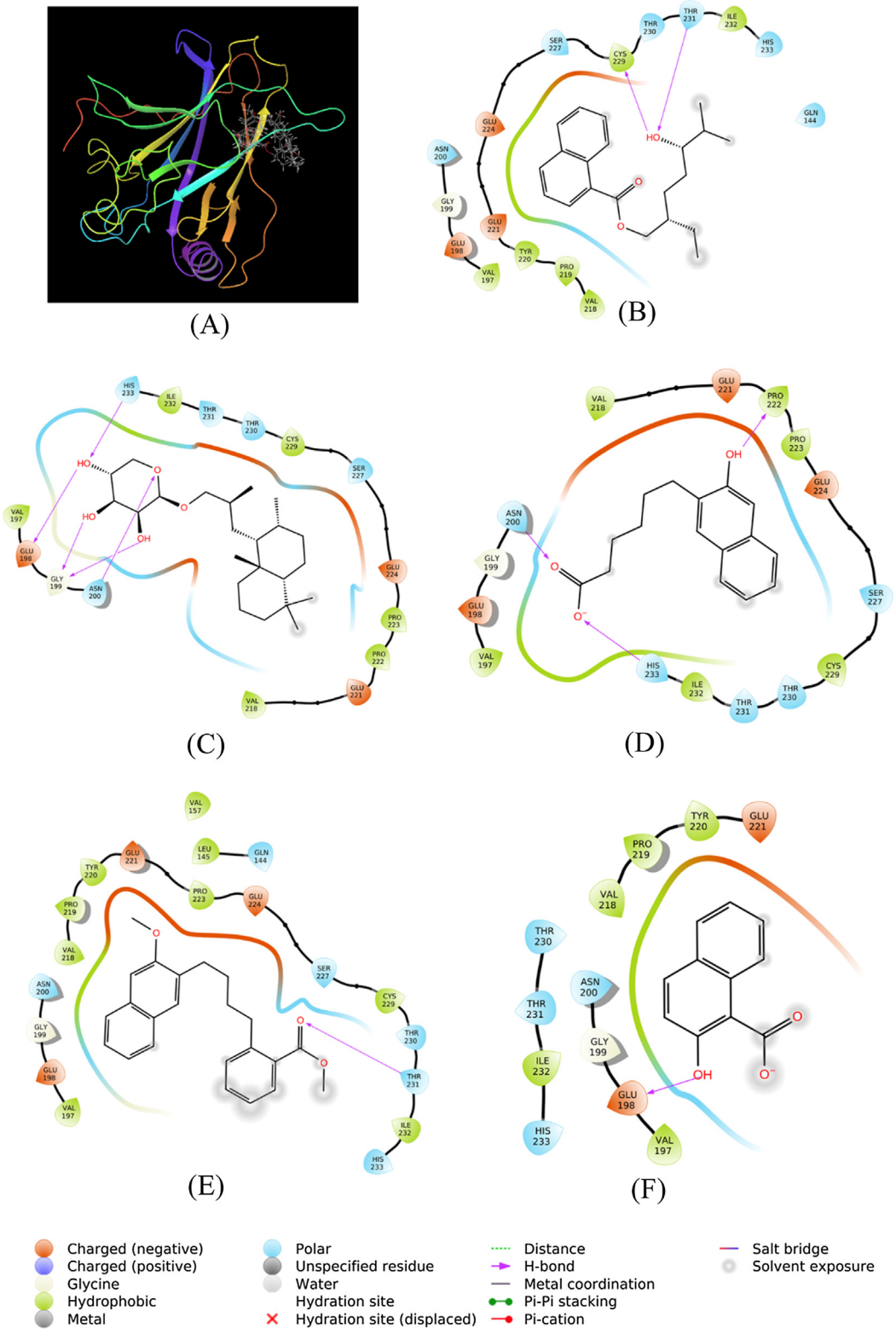

Fig. 8. Binding of SMC compounds at site 1of P53. Binding of (A) all SMC compounds, (B) SMC-1, (C) SMC-2, (D) SMC-3, (E) SMC-4, (F) SMC-5.

binding affinity of SMC-5 towards p53 were estimated to be −5.793 kcal/mol and 1.77 × 10^4 M^{-1} respectively (Table 2).

The results of molecular docking suggest that SMC compounds bind different amino acid residues of distinct domains of p53 with binding affinity in the range of 10^4-10^5 M^{-1} (Table 2). It is noticeable that the amino acid residues of binding sites I and II such as Ser99, Thr170, Gly199 and Asp224 have been reported to participate in the formation of active tetrameric form of p53 (AlAjmi et al., 2018). On the other hand, Arg280, which is located in binding site III of p53, has been shown to participate in the formation of p53-DNA complex. The binding of SMC compounds to p53 thus may prevent it to bind to DNA and thus preclude the recruitment

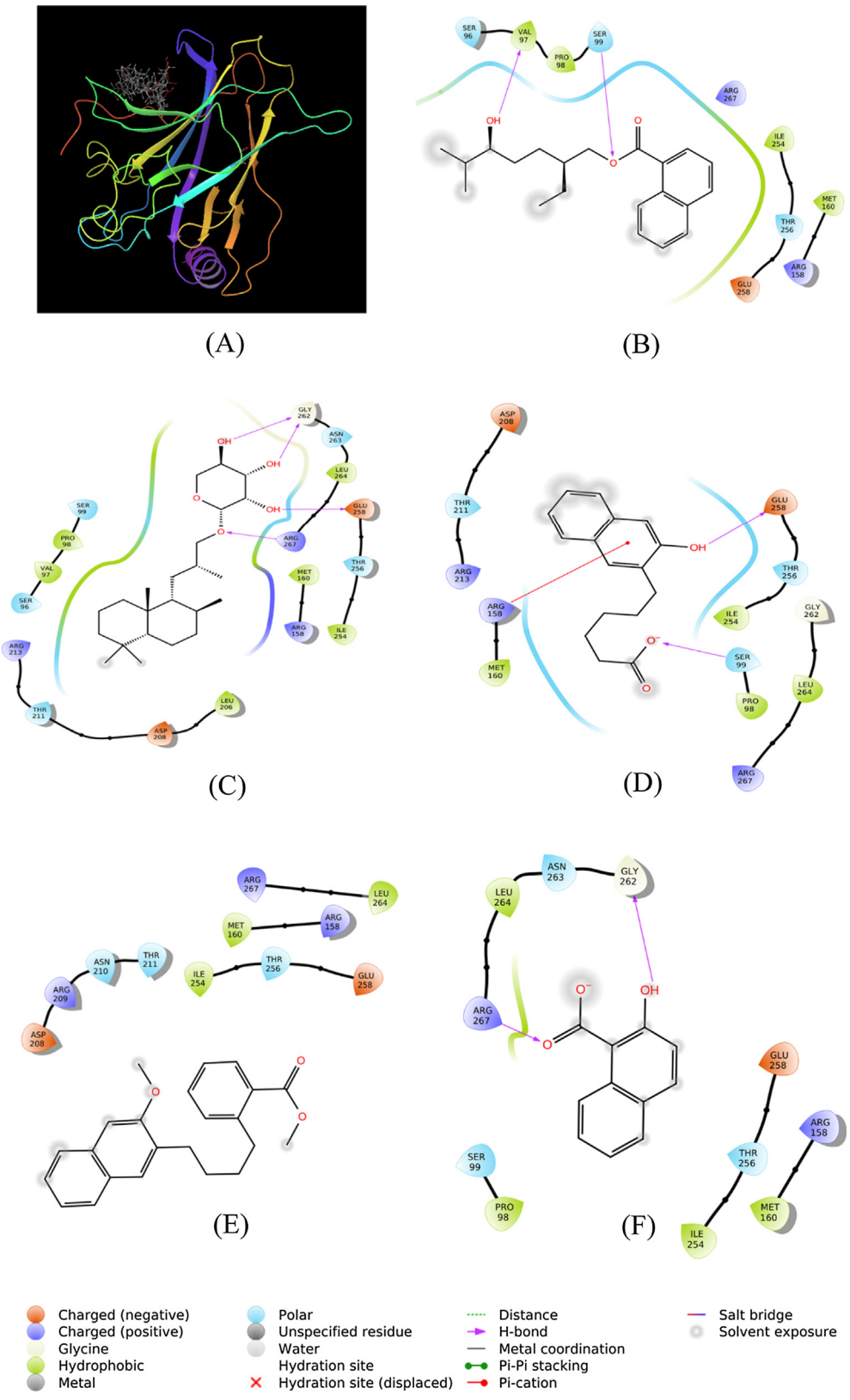

Fig. 9. Binding of SMC compounds at site 2 of P53. Binding of (A) all SMC compounds, (B) SMC-1, (C) SMC-2, (D) SMC-3, (E) SMC-4, (F) SMC-5.

of other factors necessary for cell cycle arrest. Moreover, SMC compounds may change the p53 binding activity towards its downstream targets and thus may induce aberrant cell proliferation (Bai and Zhu, 2006).

4. Conclusion

The DCM fraction of the *S. monoica* was found to be the most active in cell proliferation. The chromatographic purification of

DCM faction led to the isolation of four new compounds along with one known with remarkable cell proliferative potential (1.42–1.48 fold), which supports the use of *S. monoica* as folklore medicine for wound healing. The *in vitro* results of this study confirm that SMC compounds **(SMC 1–5)** have the potential to induce cellular proliferation in HepG2 cells. Moreover, an insight into the possible mechanism of SMCs action through molecular docking revealed that the isolated SMC compounds are able to bind and inactivate or modulate the tumor suppressor proteins such as PTEN and p53. The exact mechanism of cell proliferation by *S. monoica* need to be explored in further studies but the findings of this research justifies the use of *S. monoica* in traditional medicines.

Acknowledgement

The authors extend their appreciation to the Deanship of Scientific Research at King Saud University, Riyadh, Saudi Arabia for funding the work through the research group project number (RGP-073).

Declaration of Competing Interest

The authors declare that they don't have any conflict of interest.

References

AlAjmi, M.F., Rehman, M.T., Hussain, A., Rather, G.M., 2018. Pharmacoinformatics approach for the identification of Polo-like kinase-1 inhibitors from natural sources as anti-cancer agents. Int. J. Biol. Macromol. 116, 173–181.

Al-Hassan HO., 2006. Wild Plants of the Northern Region. Ministry of Agriculture, Camel and range research center in collaboration with FAO, Al-Jouf, SA.

Ali, A., Jameel, M., Ali, M., 2014. New naphthyl esters from the bark of *Ficus religiosa* Linn. The Nat. Prod. J. 4 (4), 248–253.

Ali, M., 2001. Techniques in Terpenoid Identification, Birlas Publications (Regd.), Shahdara, Delhi, pp. 15–23.

Al-Massarani, S.M., El-Gamal, A.A., Parvez, M.K., Al-Dosari, M.S., Al-Said, M.S., Abdel-Kader, M.S., Basudan, O.A., 2017. New Cytotoxic seco-type triterpene and labdane-type diterpenes from *Nuxia oppositifolia*. Molecules 22 (3), 389.

Al-Said, M.S., Siddiqui, N.A., Mukhair, M.A., Parvez, M.K., Alam, P., Ali, M., et al., 2017. A novel monocyclic triterpenoid and a norsesquaterpenol from the aerial parts of *Suaeda monoica* Forssk. ex J.F. Gmel with cell proliferative potential. Saudi Pharm. J. 25 (7), 1005–1010.

Ashtiani, A., Aghaei, M., Ehsani, A., Rastegar, H., Salout, M.Y., 2012. Combination of herbal extracts and platelet rich plasma induced dermal papilla cells proliferation Involvement of ERK and AKT pathway. Res. Pharm. Sci. 7 (5), 23–27.

Aslam, M., Ali, M., Dayal, R., Javed, K., 2012. Coumarins and a naphthyl labdanoate diarabinoside from the fruits of *Peucedanum grande*. C. B. Clarke, Z. Naturforsch. 67 c, 580–586.

Bai, L., Zhu, W.-G., 2006. p53: structure, function and therapeutic applications. J. Cancer Mol. 2 (4), 141–153.

Bandaranayake, W.M., 1998. Traditional and medicinal uses of mangroves. Mangroves Salt Marshes 2 (3), 133–148.

Bickford, P.C., Tan, J., Shytle, R.D., Sanberg, C.D., El-Badri, N., Sanberg, P.R., 2006. Nutraceuticals synergistically promote proliferation of human stem cells. Stem Cells Dev. 15 (1), 118–123.

Boulos, L., 1991. Notes on *Suaeda* Forssk. ex Scop. Studies in the Chenopodiaceae of Arabia: 2. Kew Bull. 46 (2), 291–296.

Boulos, L., 1999. Flora of Egypt vol. 1, 417.

Chandrasekaran, M., Kannathasan, K., Venkatesalu, V., 2008. Antimicrobial activity of fatty acid methyl esters of some members of Chenopodiaceae. Z. Naturforsch. C 63 (5–6), 331–336.

Chowdhury, P.P., Sarkar, J., Basu, S., Dutta, T.D., 2014. Metabolism of 2-hydroxy-1-naphthoic acid and naphthalene via gentisic acid by distinctly different sets of enzymes in *Burkholderia* sp. strain BC1. Microbiology 160 (Pt 5), 892–902.

Chen, Y., Zhang, X., Dantas Machado, A.C., Ding, Y., Chen, Z., Qin, P.Z., et al., 2013. Structure of p53 binding to the BAX response element reveals DNA unwinding and compression to accommodate base-pair insertion. Nucl. Acids Res. 41 (17), 8368–8376.

Collenette, S., 1999. Wildflowers of Saudi Arabia: National Commission for Wildlife Conservation and Development (NCWCD). Riyadh, SA.

Demetzos, C., Dimas, K., 2001. Labdane-type diterpenes: Chemistry and biological activity. Stud. Nat. Prod. Chem. 25, 235–292.

Elsayed, S.A., El-Hendawy, A.M., Butler, I.S., Mostafa, S.I., 2013. New complexes of 2-hydroxy-1-naphthoic acid and X-ray crystal structure of [Pt(hna)(PPh3)2]. J. Mol. Struct. 1036, 196–202.

Elsharabasy, F.S., Metwally, N.S., Mahmoud, A.H., Soliman, M.S., Youness, E.R., Farrag, A.H., Arafa, S., 2019. Phytoconstituents and hepatoprotective effect of *Suaeda monoica* Forssk and Suaeda pruinosa Lang. Biomed. Pharmacol. J. 12 (1), 117–129.

Hasan, N., Al Sorkhy, M., 2014. Herbs that promote cell proliferation. Int. J. Herb Med. 1 (6), 18–21.

Kassem, F.A., Ibrahim, H.A., El-Shazly, A.M., Abdallah, E.S.A., 2003. Plant Derived Pest Control Agents III-Insecticidal and Biochemical studies of different plant extracts against *Culex pipiens* larvae. J. Agric. Env. Sci. 2 (1), 56–68.

Kim, D.R., Kim, H.Y., Park, J.K., Park, S.K., Chang, M.S., 2013. *Aconiti Lateralis* Preparata Radix Activates the Proliferation of Mouse Bone Marrow Mesenchymal Stem Cells and Induces Osteogenic Lineage Differentiation through the Bone Morphogenetic Protein-2/Smad-Dependent Runx2 Pathway. Evid. Based Complement. Alternat. Med. 2013, 586741.

Lakshmanan, G., Rajeshkannan, C., Kavitha, A., Mekala, B., Kamaladevi, N., 2013. Preliminary screening of biologically active constituents of *Suaeda monoica* and *Sesuvium portulacastrum* from palayakayal mangrove forest of Tamilnadu. J. Pharmacog. Phytochem. 2 (3), 149–152.

Lee, C.U., Hahne, G., Hanske, J., et al., 2015. Redox Modulation of PTEN Phosphatase Activity by Hydrogen Peroxide and Bisperoxidovanadium Complexes. Angew Chem. 54 (46), 13796–13800.

Lee, J.-O., Yang, H., Georgescu, M.-M., Di Cristofano, A., Maehama, T., Shi, Y., et al., 1999. Crystal structure of the PTEN tumor suppressor: implications for its phosphoinositide phosphatase activity and membrane association. Cell 99 (3), 323–334.

Leslie, N.R., Downes, C.P., 2004. PTEN function: how normal cells control it and tumor cells lose it. Biochem. J. 382 (Pt 1), 1–11.

Padmakumar, K., Ayyakkannu, K., 1997. Antiviral activity of marine plants. Indian J. Virol. 13 (1), 33–36.

Premnathan, M., Chandra, K., Bajpai, S., Kathiresan, K., 1992. A survey of some Indian marine plants for antiviral activity. Botanica marina 35 (4), 321–324.

Premnathan, M., Nakashima, H., Kathiresan, K., Rajendran, N., Yamamoto, N., 1996. *In vitro* anti human immunodeficiency virus activity of mangrove plants. Indian J. Med. Res. 103, 278–281.

Ravikumar, S., Gnanadesigan, M., Inbaneson, S.J., Kalaiarasi, A., 2011a. Hepatoprotective and antioxidant properties of *Suaeda maritima* (L.) dumort ethanolic extract on concanavalin-A induced hepatotoxicity in rats. Indian J. Exp. Biol. 49 (6), 455–460.

Ravikumar, S., Gnanadesigan, M., Seshserebiah, J., Jacob Inbaneson, S., 2010. Hepatoprotective effect of an Indian salt marsh herb Suaeda monoica Forsk. Ex. Gmel against concanavalin-A induced toxicity in rats. Life Sci. Med. Res. 2010 (LSMR-2), 1–9.

Ravikumar, S., Ramanathan, G., Inbaneson, S.J., Ramu, A., 2011b. Antiplasmodial activity of two marine polyherbal preparations from *Chaetomorpha antennina* and *Aegiceras corniculatum* against *Plasmodium falciparum*. J. Parasitol. Res. 108 (1), 107–113.

Sy, L.-K., Brown, G.D., 1997. Labdane diterpenoids from *Alpinia chinensis*. J. Nat. Prod. 60 (9), 904–908.

Yezhelyev, M.V., Gao, X., Xing, Y., Al-Hajj, A., Nie, S., O'Regan, R.M., 2006. Emerging use of nanoparticles in diagnosis and treatment of breast cancer. Lancet Oncol. 7 (8), 657–667.

Zdzisińska, B., Rzeski, W., Paduch, R., Szuster-Ciesielska, A., Kaczor, J., Wejksza, K., Kandefer-Szerszeń, M., 2003. Differential effect of betulin and betulinic acid on cytokine production in human whole blood cell cultures. Pol. J. Pharmacol. 55 (2), 235–238.

Zheng, C.-J., Lan, X.-P., Wang, Y., Huang, B.-K., Han, T., Zhang, Q.-Y., Qin, L.-P., 2012. A new labdane diterpene from *Vitex negundo*. Pharm. Biol. 50 (6), 687–690.